Chemical Composition of Hexene Based LLDPE by Infrared Spectroscopy and Chemometrics

Olivier Boyron, Manel Taam, Christophe Boisson*

Université de Lyon, Univ. Lyon 1, CPE Lyon, CNRS UMR 5265, Laboratoire de Chimie Catalyse Polymères et Procédés (C2P2), Equipe LCPP, Bat 308F, 43 Bd du 11 Novembre 1918, F-69616 Villeurbanne, France

E-mail : olivier.boyron@univ-lyon1.fr

Keywords: infrared; near infrared; ethylene-1-hexene copolymer; LLDPE; chemometrics

Abstract

Mid and near infrared (MIR and NIR) spectroscopy associated with the partial least squares (PLS) method makes it possible to rapidly characterize the composition of linear low-density polyethylene (LLDPE) in a large range of 1-hexene content from 0 to 21 mol%. LLDPEs are produced using zirconocene catalysts activated with methylaluminoxane. PLS regression methods for MIR and NIR are constructed from this series of LLDPEs to quantify the 1-hexene content in unknown copolymers. In this case, the PLS regression method aims to correlate the 1-hexene content in the copolymers with their IR spectra. Multivariate calibration models are constructed by the PLS algorithm on pretreated data of MIR and NIR analyses. They are tested and validated by comparing results obtained by NMR and the PLS analyses for four unknown ethylene-1-hexene copolymers.

1. Introduction

With an annual global production of approximately 100 million tons, polyethylenes (PEs) are the main commercial polymeric materials.[1, 2] They are typically classified into three main families such as high-density polyethylene (HDPE; 0.940 to 0.970 g/cm3), low-density polyethylene (LDPE; 0.910 to 0.940 g/cm^3) and linear low-density polyethylene (LLDPE; 0.916 to 0.940 g/cm^3). HDPE has no or only a small amount of branching (SCB), LDPE contains a combination of long (>C_6) and short chain branching, while the branching in LLDPE is predominantly from short chain branching. This last one is synthetized by copolymerization of ethylene and an α-olefin which allows the insertion of a short-chain branching into the main chain and thus impacts the crystallinity of the material.[3] The frequently used α-olefins are 1-butene, 1-hexene and 1-octene.[1, 4] The crystallinity and then the physical properties of LLDPE can be adjusted using different content of comonomer.[5, 6] Consequently, it is highly relevant to quantify the amount of comonomer units incorporated into LLDPE during the polymerization process.

Various analytical techniques have been developed to quantify the short chain branching content. It has been widely investigated using spectroscopy like Fourier transform infrared (FTIR)[7-10], proton and carbon nuclear magnetic resonance (H-NMR and ^{13}C-NMR)[11-14]. Liquid chromatography based on crystallibility of polyolefins has been established by Wild, Monrabal, Soares and Pasch through temperature rising elution fractionation (TREF)[15-19] and crystallization analysis fractionation (CRYSTAF)[20, 21]. However, these techniques cannot be used for the separation of amorphous fractions of the polymers. The combination of high temperature liquid chromatography with a Hypercarb column operating with a temperature gradient [22-27] was introduced by Cong and Macko and allow the analysis of amorphous polymers. These high temperature fractionation techniques were able to determine the chemical composition distribution (CCD) of LLDPE. In addition, thermal analysis coupled with mass

spectrometry[28-31] has been employed to measure the branching type and the content of α-olefins in LLDPE.

However, these approaches are time consuming due to the sample preparation (dissolution at high temperature with toxic solvent) for most techniques and the time required to record and process the data. In many instances, for example in the case of high throughput experiments or during recycling process, it is desirable to determine the polymer composition in a shorter time. Infrared spectroscopy is a consistent and an essential analytical method for exploring polymer composition.[32, 33] More specifically, Fourier transform infrared spectroscopy in attenuated total reflection mode (ATR-FTIR)[34-36] and near infrared (NIR)[37-39] equipped with an integrating sphere might be advantageous for measuring the chemical composition of LLDPE as inexpensive sample preparation is sufficient for theses technique. While many previous studies[9, 40, 41] are based on absorbance attributable to branch type there are few publications on quantitative studies.[7, 42, 43] In work of Blitz and McFaddin,[7] FTIR calibration for different branch type (methyl, ethyl, butyl, hexyl) in LLDPE based on absorption of only one wavelength was reported. Sano et al and Shimoyama et al described methods to predict density in LLDPE by applying chemometrics tools to Raman spectra[42] and near IR spectra[43]. In this present study we propose to calibrate IR analysis of LLDPE with a large and complete set of polymers up to 21 mol% of 1-hexene and with multiple absorption bands in order to increase the robustness and precision of the method.

Because structural changes in ethylene-1-hexene copolymers cause low modifications in MIR and NIR spectra, the use of chemometrics techniques are required to highlight differences in polymer spectra. Partial least-squares (PLS) regression is commonly used to improve the resolution in analytical signals that can be overlaid for intricate materials.[44-48] In particular, we demonstrated, in a previous work, that PLS regression can be efficiently used for quantitative determination of composition of ethylene-butadiene copolymers.[49]

This work proposes an original method based on infrared spectroscopy and chemometrics. Firstly, copolymers containing various proportions of 1-hexene were synthetized using the zirconocene catalyst.[50-52] Secondly, the average composition of the copolymers was measured using ^{1}H and ^{13}C-NMR spectroscopy. The homogeneity in molar mass and chemical composition was also controlled by high temperature size exclusion chromatography (HT-SEC) and thermal gradient interaction chromatography (TGIC). Subsequently, the copolymers were used to construct the PLS model with NIR and MIR data.

2. Experimental Section

2.1. Polymerization method

All manipulations were performed under dry argon, using standard Schlenk techniques and glovebox. 1-hexene was dried over CaH_2 prior to use. Toluene and heptane were dried on 3 Å molecular sieves. Methyl-aluminoxane (MAO) 10% wt. in toluene was purchased from Aldrich and triethylaluminium ($AlEt_3$) was purchased from Albemarle and used as heptane solution (1 M). Ethylene (99.5%) from Air Liquide was purified by passing on three successive columns containing respectively molecular sieves, alumina and a copper catalyst. The metallocene complexes rac-Et$(Ind)_2ZrCl_2$ and $(nBuCp)_2ZrCl_2$ were purchased from Sigma-Aldrich. The activating support was prepared as described in previous work.[53]

Ethylene polymerizations were performed in a 500 ml glass reactor equipped with a stainless-steel blade stirrer and an external water jacket to control the temperature. MAO and the required amounts of 1-hexene were introduced in a flask containing 300 mL of heptane. The mixture was transferred in the reactor under a stream of argon. The argon was then pumped out before introducing the ethylene or a mixture of ethylene/propene. Temperature and pressure were then progressively increased up to 80 °C and 3.8 x 10^5 Pa. 100 µL of a solution (1.5 mM in toluene) of rac-Et$(Ind)_2ZrCl_2$ and $(nBuCp)_2ZrCl_2$ were then introduced in the reactor under 4 x 10^5 Pa

of ethylene to start the polymerization. The pressure was kept constant at 4 x 10^5 Pa during the polymerization. After 30 minutes of reaction, the polymerization was stopped by releasing the pressure and cooling down the reactor to the room temperature. The resulting mixture was poured in 400 mL of methanol. The polymer was collected by filtration, washed with methanol and dried under vacuum.

In the case of slurry polymerization using the supported rac-Et$(Ind)_2ZrCl_2$ catalyst, a similar procedure was used. However the Al(i-Bu)$_3$ (1 M solution in heptane), the activating support, the metallocene precatalyst (1 mM solution in toluene), and 1-hexene were introduced successively in the flask containing 300 mL of heptane. The mixture was transferred in the reactor and the polymerization started by pressurization of the reactor to 4 x 10^5 Pa.

2.2. Characterization

2.2.1. High temperature size exclusion chromatography

High temperature size exclusion chromatography (HT-SEC) analyses were performed using a Viscotek system, from Malvern Instruments, equipped with a combination of three columns (PLgel Olexis from Agilent Technologies, 300 mm × 7.5 mm, 13µm). Samples were dissolved in 1,2,4-trichlorobenzene (TCB) with a concentration of 5 mg mL^{-1} by heating the mixture for 1 h at 150°C. 200 µL of sample solutions were injected and eluted with 1,2,4-TCB using a flow rate of 1 mL min^{-1} at 150 °C. 2,6-di-tert-butyl-4-methylphenol (BHT) was added to the eluent (200 mg L^{-1}) in order to stabilize the polymer against oxidative degradation. Online detection was performed with a differential refractive-index detector and a dual light-scattering detector (LALS and RALS) for absolute molar mass determination. OmniSEC software version 5.2 was used for data acquisition and calculation.

2.2.2. Thermal Gradient Interaction Chromatography

TGIC experiments were performed using an instrument from PolymerChar (Valencia, Spain) to characterize the composition distribution in samples. The instrument was equipped with a Hypercarb column from Thermo Scientific. The samples were dissolved in 10 mL vials for 1 h at 150 °C with 1,2,4 trichlorobenzene (TCB) containing 300 ppm of BHT and purge with nitrogen to protect the polymer against oxidative degradation. 200 µL of sample solution at a concentration of 1 mg mL^{-1} were injected into the column at 150 °C. This technique requires a cooling (adsorption) and a heating (desorption) step. A cooling ramp of 20 °C min^{-1} down to 40 °C was applied to promote polymer adsorption. Elution begins isothermally at 40 °C during 5 min at a flow rate of 0.5 mL min^{-1} followed by a heating ramp at 2 °C min^{-1} to desorb the polymer. An infrared detector was used to monitor the components' concentration and composition when the chains were eluted from the column.

Because TGIC separates by adsorption it has the possibility to extend the range of polymers to be analyzed towards the amorphous region which is limited by crystallization techniques (TREF, CRYSTAF). Then, LLDPE with high content of comonomer can be separated.

2.2.3. Nuclear magnetic resonance spectroscopy

Co-monomer contents of copolymers were determined by NMR using a Bruker Avance III 400 spectrometer operating at 400 MHz for ^{1}H-NMR and 100.6 MHz for ^{13}C-NMR. ^{1}H-NMR spectra were obtained with a 5mm QNP probe at 373 K and the ^{13}C-NMR spectra were obtained with a 10 mm PA-SEX probe at 373 K. A 3:1 volume mixture of 1, 2, 4-trichlorobenzene and toluene-d8 was used as solvent. The chemical shifts were measured in ppm using for ^{1}H-NMR the reference of toluene (CHD_2 at 2.185 ppm) and for ^{13}C-NMR the resonance of the major backbone methylene carbon resonance (CH_2 at 30.00 ppm) as internal references.

2.2.4. Mid infrared spectroscopy

Mid infrared (MIR) spectra were recorded using a Nicolet iS50 Fourier transform infrared (FTIR) spectrometer from Thermo Fisher Scientific. The spectrometer was equipped with an attenuated total reflection (ATR) module (single-bounce diamond crystal) and a deuterated triglycine sulfate detector and KBr optics. Before each measurement, the diamond crystal was carefully cleaned with ethanol and dried in ambient air. A small amount of sample in powder state was pressed directly on the diamond crystal with a constant pressure of 7 x 10^7 Pa. Background and sample were acquired using 32 scans at a spectral resolution of 4 cm^{-1} from 4 000 to 400 cm^{-1}. Spectral data were obtained with OMNIC Software from Thermo Fisher Scientific. The ATR spectra were not corrected for pathlength. Three replicates for each sample were made and compared. If they were similar, only one spectrum was selected and used for the model. They were different for one sample and it was not used in this work.

2.2.5. Near infrared spectroscopy

Near infrared (NIR) spectra were collected using a Nicolet iS50 FTIR spectrometer from Thermo Fisher Scientific under nitrogen. The spectrometer was equipped with an integrating sphere (Thermo Scientific Smart NIR).

The synthetized LLDPE gives, for some of them, a heterogeneous powder agglomeration. Working on the raw samples was difficult and a second method using a solvent to dissolve samples was also performed. To obtain a homogenous solution, 40 mg of polymer in 200 µL of 1,2,4-TCB, with BHT as stabilizer, was dissolved in a 2 ml vial. Then the vials were heated up to 150 °C for 1 hour in order to entirely dissolve the sample. Since glass does not absorb in NIR the samples were analyzed directly through the vials.

Background and samples were acquired using 32 scans at a spectral resolution of 4 cm^{-1} from 11 000 to 3 800 cm^{-1}. Spectral data were obtained with OMNIC Software from Thermo Fisher Scientific.

2.2.6. Chemometrics tools

Chemometric analyse of NIR and MIR spectra were achieved using a partial least squares (PLS) method with two different softwares. TQ Analyst software from Thermo Fisher Scientific and The Unscrambler X 10.5.1 software from Camo were used to analyze NIR and MIR data, construct the models and quantify the unknown samples.

3. Results and discussion

3.1. Chemical composition of ethylene-1-hexene copolymers

The present work was developed to determine 1-hexene content in LLDPE in a straightforward way. The copolymerization of ethylene with 1-hexene using metallocene catalysts provides polymers with various comonomer content (**Scheme 1**).

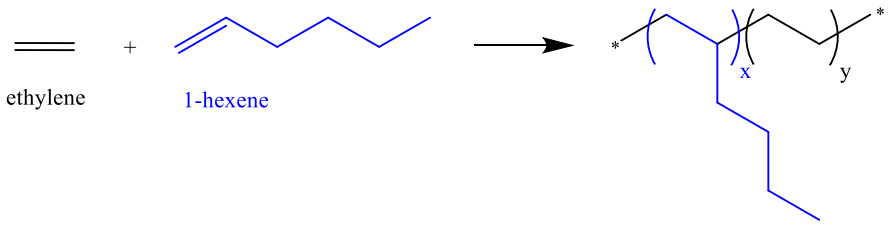

Scheme 1. Chemical structure of ethylene-1-hexene copolymers

A vast set of ethylene-1-hexene copolymers (**Table 1**) was obtained by changing comonomer content during synthesis. The catalyst used in this work led to polymers with the controlled molecular structure in molar mass and in comonomer composition. They were analysed by HT-SEC, TGIC and NMR before using them to construct the PLS models.

Table 1. Characterization of ethylene-1-hexene copolymers obtained with zirconocene catalyst.

Sample	**Cata[a]**	**Mn (Đ)[a] kg.mol^{-1}**	**Hex[c] mol%**	**Tp[d] °C**	**Hex[d] mol%**	**Cw/Cn[d]**
1	1	60 (2.9)	**0.0**	132.5	0.1	2.5
2	1	51 (3.2)	**0.0**	132.5	0.0	2.5
3	1	50 (3.4)	**0.0**	*nd*	*nd*	*nd*
4	1	44 (3.0)	**0.0**	*nd*	*nd*	*nd*

5	1	51 (3.1)	**0.0**	*nd*	*nd*	*nd*
6	2	49 (3)	**0.2**	132.0	0.3	3.0
7	1	41 (3.8)	**0.3**	131.7	0.3	2.0
8	1	21 (2.2)	**0.4**	130.8	0.2	1.3
9	2	24 (3.4)	**0.5**	131.0	0.4	3.0
10	3	36 (3.1)	**0.7**	*nd*	*nd*	*nd*
11	3	48 (2.6)	**0.7**	130.8	0.7	1.1
12	3	33 (4.1)	**1.0**	130.5	0.6	1.2
13	1	40 (2.6)	**1.1**	*nd*	*nd*	*nd*
14	3	29 (4.7)	**1.1**	*nd*	*nd*	*nd*
15	3	51 (2.2)	**1.2**	129.4	0.9	2.0
16	2	52 (3.1)	**1.5**	126.9	1.2	2.0
17	3	56 (2.3)	**1.5**	*nd*	*nd*	*nd*
18	1	54 (2.6)	**1.6**	*nd*	*nd*	*nd*
19	3	25 (3.7)	**1.8**	129.4	0.7	1.4
20	2	56 (3.1)	**1.9**	128.7	1.2	1.1
21	1	36 (1.8)	**2.0**	124.3	1.8	1.6
22	2	35 (2.3)	**2.0**	*nd*	*nd*	*nd*
23	1	40 (1.7)	**2.2**	123.1	2.1	1.3
24	1	40 (2)	**2.2**	*nd*	*nd*	*nd*
25	1	28 (2.2)	**2.2**	*nd*	*nd*	*nd*
26	3	42 (2.3)	**2.3**	*nd*	*nd*	*nd*
27	1	40 (1.9)	**2.5**	121.8	2.5	1.2
28	1	40 (2.2)	**2.5**	*nd*	*nd*	*nd*
29	3	56 (2.3)	**3.0**	*nd*	*nd*	*nd*
30	1	24 (2.9)	**3.0**	*nd*	*nd*	*nd*
31	3	40 (2.1)	**3.6**	114.4	4.2	1.5
32	3	26 (2.6)	**3.7**	117.8	4.0	1.4
33	3	22 (3.7)	**3.9**	116.7	3.8	1.3
34	3	24 (2.9)	**4.1**	114.7	4.1	1.1
35	1	41 (1.8)	**5.3**	107.8	5.8	1.1
36	1	46 (2)	**5.6**	105.7	6.3	1.1
37	1	37 (1.8)	**6.3**	102.7	7.0	1.1
38	1	40 (2.1)	**7.0**	98.9	7.8	1.0

39	1	60 (4.1)	**9.0**	*nd*	*nd*	*nd*
40	1	56 (2)	**13.6**	77.4	13.1	1.2
41	1	31 (1.4)	**20.7**	53.6	19.0	1.0

[a] catalytic systems based on the complexes [1] rac-Et(Ind)$_2$ZrCl$_2$ and [2] (nBuCp)$_2$ZrCl$_2$ [3] supported rac-Et(Ind)$_2$ZrCl$_2$ used for the preparation of ethylene-1-hexene samples.[b] Number average molar mass and dispersity obtained with HT-SEC, [c] 1-hexene content determined with ^{1}H NMR and ^{13}C NMR, [d]elution peak temperature, 1-hexene content and dispersity of chemical composition obtained by TGIC, [nd] not determined

3.2. Interpretation of NMR spectra

^{13}C NMR spectra was used to determine and quantify the chemical composition of homopolymers and copolymers with a 1-hexene content below 4% (**Figure 1**). The ^{13}C NMR spectra of highly branched linear low-density polyethylene is tricky and requires a detail analysis of monomer sequences.[54] In that case ^{1}H-NMR was used to provide reliable 1-hexene content since the signal of methyl chain end can be neglected. Calculation of 1-hexene content has been reported in a previous work.[18]

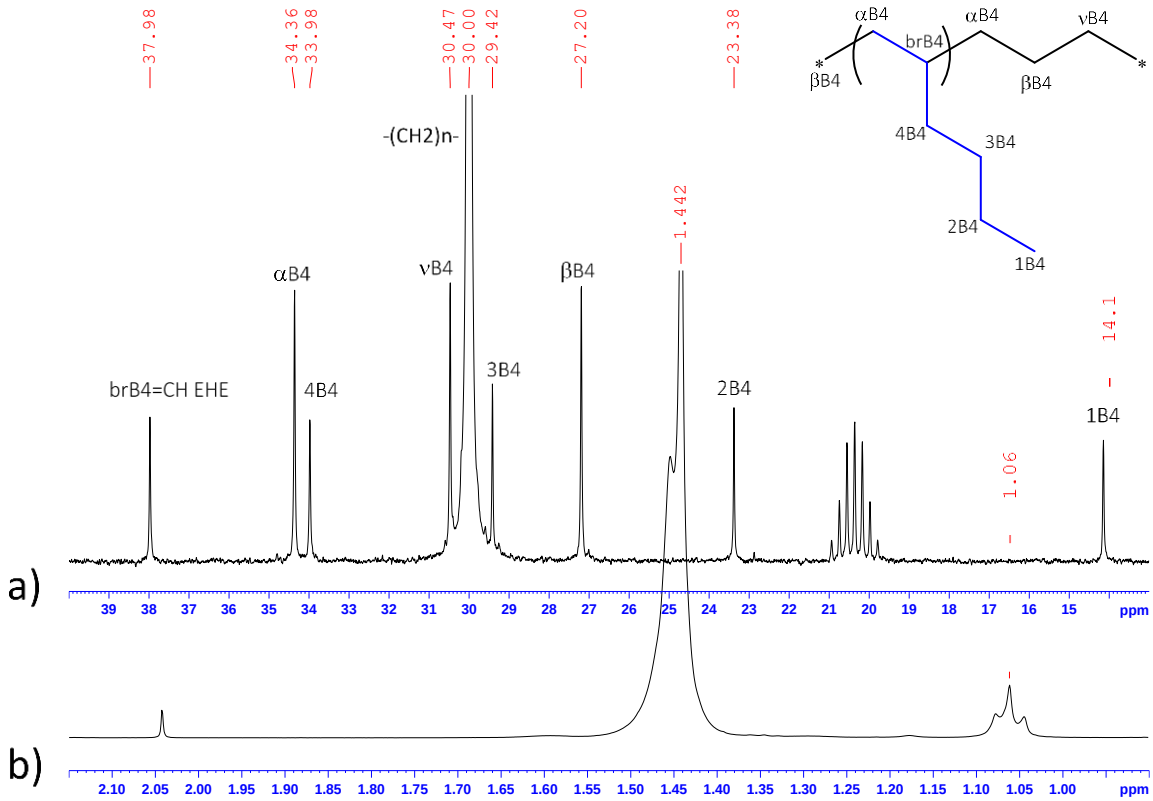

Figure 1. ^{13}C NMR spectra (TCB/ toluene-d8, 363 K) of sample 23 with 2,2 mol% of 1-hexene, a), resonance region of ^{1}H NMR spectra (TCB/ toluene-d8, 363 K) of sample 40 with 13,6 mol% of 1-hexene b).

3.3. Chemical composition distribution

The molar masses and the dispersity of samples are reported in Table 1. The SEC profiles, in **Figure 2a**, show a unimodal molar masses distribution. The TGIC peak of the samples elutes in decreasing order of comonomer content, as observed in previous works.[24, 27, 55-58] The elution temperature of 11 samples, issue from homogeneous catalyst [1, 2] and supported catalyst [3], were plotted (**Figure 2b**). The peaks are rather narrow and have a similar distribution to a Gaussian which confirms that all polymers were quite homogeneous in composition.

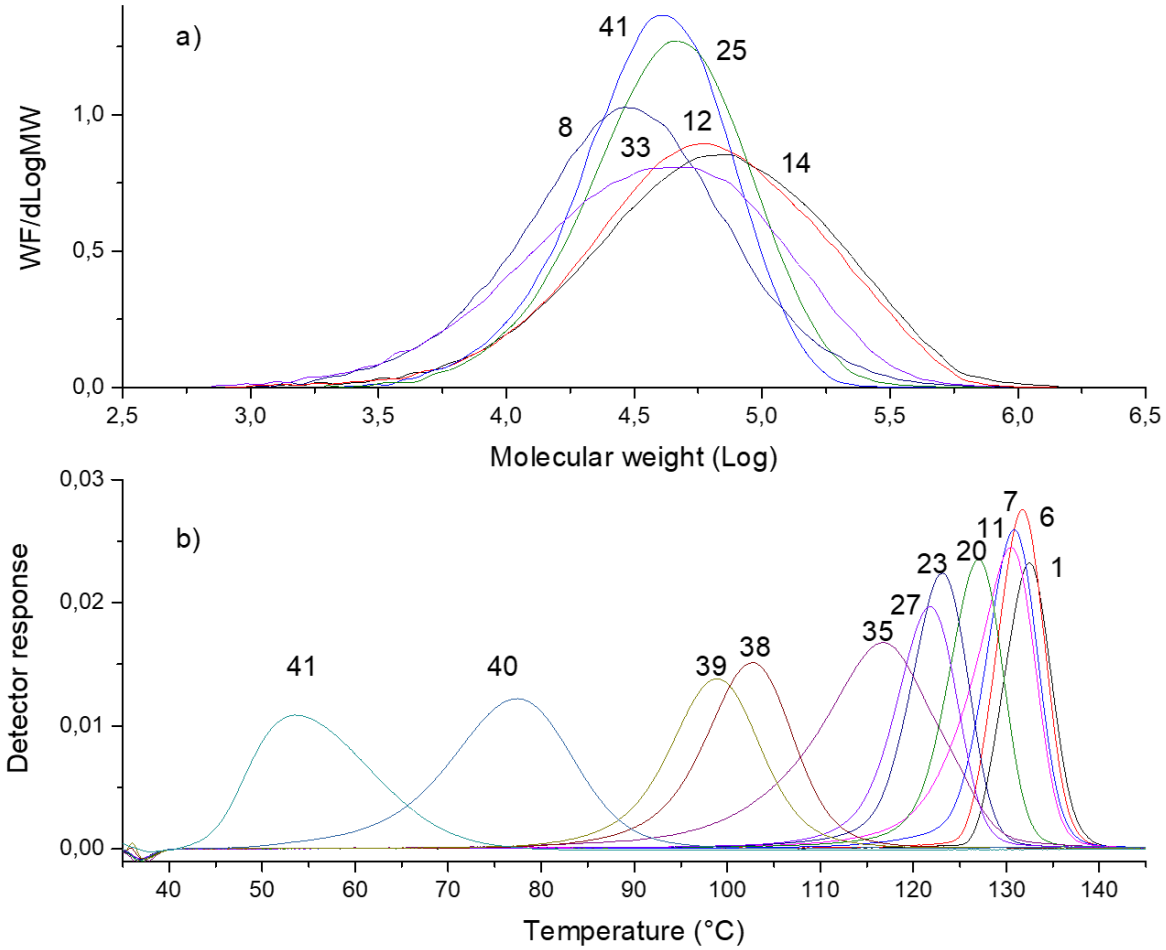

Figure 2. SEC a) and TGIC b) profiles of a set of ethylene-1-hexene copolymers ranging from 0 to 20.7 mol% of 1-hexene.

Quantifications of the 1-hexene content by TGIC were very similar to the values obtained by NMR. As NMR is a more conventional method, it has been chosen as the main reference method for developed models.

3.4. Interpretation of MIR spectra

The copolymer samples were analysed by MIR spectroscopy using ATR accesory. **Figure 3** shows the comparison of FTIR spectra of a homopolyethylene and four ethylene-1-hexene copolymers.

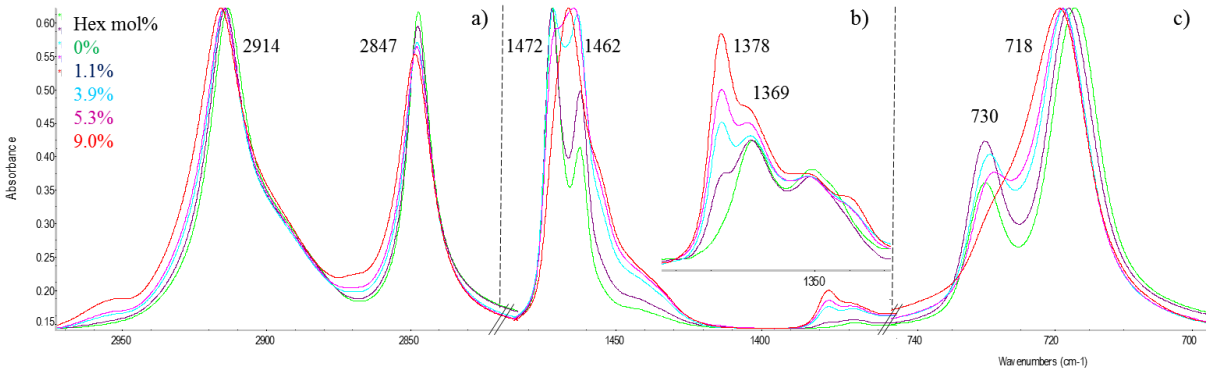

Figure 3. MIR spectra overlay of a polyethylene and four copolymers with various comonomer contents.

LLDPE showed a relatively simple infrared spectrum (Figure 3), the major absorption bands observed have been reported previously.[47, 59, 60] The IR spectra of LLDPE, containing different amount of hexene, were found to have significant differences in four different regions. Four ratios of very close bands were studied. When the comonomer content increases in the copolymer we observed that the ratio of the peak intensity 2914 cm^{-1}/2847 cm^{-1}, 1472 cm^{-1}/1462 cm^{-1} and 1378 cm^{-1}/1369 cm^{-1} increased while the ratio of the peak intensity 730 cm^{-1} /718 cm^{-1} decrease significantly.

In Figure 3b, the ratio of absorption at 1378 cm^{-1} (due to methyl groups C-H deformation) versus absorption at 1369 cm^{-1} (due to methylene group C-H deformation) clearly shows a trend with the variation of 1-hexene amount in the copolymer. For the homo-polyethylene, no absorption was observed at 1378 cm^{-1} whereas as the comonomer content increased in the copolymer, the intensity of this peak increased. The splitting of absorption bands is due to semi-crystalline properties of LLDPE as described in previous work[61]. Comonomer content has a slight impact on different parts of the IR spectrum. In order to consider all these modifications on the spectrum, the chemometric analysis was applied in this study.

3.5. Interpretation of NIR spectra

The absorption spectrum of a representative sample is shown in **Figure 4**. In agreement with previous work,[62-64] the assignments of the eight main absorption bands are reported in **Table 2**.

Table 2. Assignments of NIR bands of ethylene-1-hexene copolymers.

NIR	Wavenumber [cm-1]	Assignment	Comments
LLDPE	8600 à 8000	second harmonic oscillation of CH, CH_2,CH_3	large, medium, gaussian look
	7300 à 6800	first harmonic oscillation of CH, CH_2, CH_3	very large, medium
	7200		medium, thin
	5800 à 4800	//	elevation of the base line
	5780	first harmonic oscillation of CH, CH_2, CH_3	very intense, thin
	5620		intense, thin
	5600 à 5400		medium, large
	4400 à 4200	combination of CH, CH_2, CH_3	very intense

NIR spectra are composed of overlapping overtones and combinations of bands originating from the MIR. They contain a wealth of information on the chemical and physical properties of the copolymers. Since it was a considerable effort to deduce some characteristic of LLDPE microstructure from the spectra, the data were exploited using chemometric tools.

The spectrum of dissolved polymer (Figure 4b) were more noisy but more robust and repetitive compare to spectrum obtained with solid sample (Figure 4a). A PLS model was constructed with both kind of preparation. The NIR spectrum of the solvent, used for the sample dissolution, was acquired separately (Figure 4c).

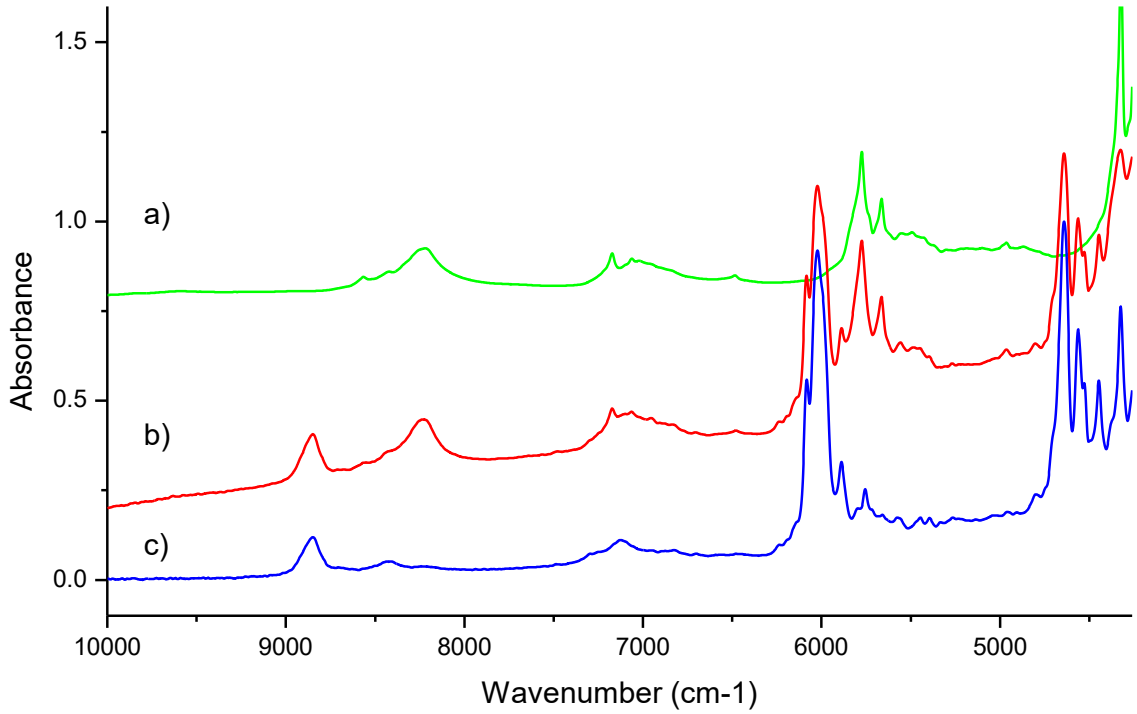

Figure 4. NIR spectra of a copolymer (sample 12) a) in solid state b) dissolved in trichlorobenzene and c) solvent alone.

3.6. Chemometric study

The goal of this work was to obtain a robust method to determine the 1-hexene content of an unknown copolymer with MIR and NIR spectroscopy. A partial least squares regression (PLS) model[44, 45, 65] was used.

3.6.1. Calibration set

In order to determine composition of an unknown ethylene-1-hexene copolymer, calibration methods for MIR and for NIR were created with a set of 41 samples described above. The wide range of composition of ethylene-1-hexene copolymers, from 0% to 20.7 mol%, was particularly interesting for this purpose.

3.6.2. Performance index

The performance index (PI), that indicates the adequacy between the calculated polymer compositions and NMR measurements, was chosen to measure the accuracy of the method. The

higher the performance index (up to 100) is, the better the agreement between calculated and NMR values are. This parameter, reported for each method in Table 4, allowed us to decide whether the modifications of the pre-processing data improve the accuracy of the method.

3.6.3. Prediction performance

The performance of the model was evaluated with the root mean square error of calibration (*RMSEC)*, the root mean square error of validation (*RMSEV)* and the correlation coefficient (r). These values were reported in Table 4.

RMSEC (mol%) corresponds to the error calculated using the standards and was calculated with **Equation 1**:

$$RMSEC = \sqrt{\sum_{i=1}^{N}(\hat{y}_i - y_i)^2 / (N - A - 1)} \qquad \textbf{(1)}$$

RMSEV (mol%) was calculated with a cross validation method. The Kernel algorithm[46-48] was selected. It can be expected to perform well in our case with data containing many samples and few variables. A sample was removed from the calibration set and predicted with a model created with the remaining samples. The procedure was repeated by omitting each of the samples from the calibration set. RMSEV value was a measure of the average uncertainty that could be expected when predicting new samples, and was calculated with **Equation 2:**

$$RMSEV = \sqrt{\sum_{i=1}^{N_p}(\hat{y}_i - y_i)^2 / (N_p)} \qquad \textbf{(2)}$$

N = number of samples; N_p = number of samples in prediction set; $\hat{y}_i$ = model predicted value for sample i; A = number of PLS factors in model;

- r^2: the correlation coefficient between predicted and measured value is a measure of the quality of the model. The closer to 1, the better is the model. For the calibration, r_c represents the quality of the fit. For validation, r_v characterizes the predictive ability of the model.

In order to validate the model, RMSEC and RMSEV values must be low and similar and r^2 close to one.

3.6.4. Number of factors in PLS regression

The performance index plot was used to measure the divergence between the model and actual data. It allows the determination of the PLS factor number (Table 4) to be used to properly describe the variables. As the number of PLS factors increased, the performance index plot increase. When the curve reaches its maximum, this value corresponds to the optimum number of PLS factors. Including more PLS factors, the model will fit the calibration set better but can lead to an 'over-fitting' of the model and to a poorer prediction for unknown sample. The choice of four factor number in the calibration model was a balance between optimizing the explain variance and limiting the model complexity.

3.6.5. Preprocessing method

Several data pre-processing methods were applied. The first derivate of the NIR and MIR signals was chosen in order to reduce the baseline offset and the instrumental drift. In the derivation process, noise can increase which requires a smoothing. The Savitzky-Golay algorithm[66-68] was used for smoothing the signal and to reduce the impacts of varying baseline, variable path lengths, and high stray lights due to scatter effects. A polynomial order of 2 and a segment length of 7 points were applied. The pre-processing method was applied both to the whole spectrum and to the spectral region selection.

3.7. Scores

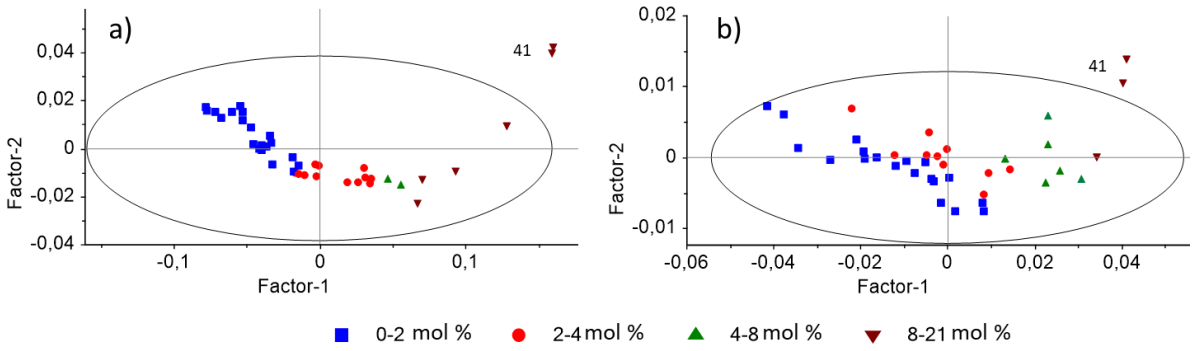

Figure 5. A principal component analysis (PCA) scores for factor 1 and factor 2 with confidence intervals of 95% of a) MIR and b) NIR for ethylene-1-hexene copolymers sample. Samples were disctinctly separated into four groups (blue, red, green and brown) depending of 1-hexene content (in mol%).

A principal component analysis (PCA) scores for factor 1 and factor 2, in **Figure 5**, summarized more variation in the data than any other pair of components. The closer the samples were in the score plot, the more similar they were. The plot for MIR (Figure 5a) and for NIR (Figure 5b) shows that when 1-hexene content increase, from blue to brown, the sample was clearly shifted to the right. This means that the amount of comonomer had a real impact on the spectra and that it could be measure using PLS regression. The scores plot shows that the separation of the four regions of different hexene levels was better for the MIR model than for the NIR model. The both score plot show that the sample 41 was considered as outlier. This sample was different from the others, not because of an analytical error, but because of the high amount of hexene. It was considered a false outlier and was not removed to preserve the large range of analyses. Sample 41 was analyzed and used twice in the model to give more weight to this sample which is located alone at the end of the calibration. In addition, the sigmoid-shaped curvature of the score plots indicates that there were interactions between the predictors. Adding more factor to the model would improve it.

3.7.1. Spectral region selection

One approach was based on spectral region selection in which the wavelength with low correlation were eliminated.

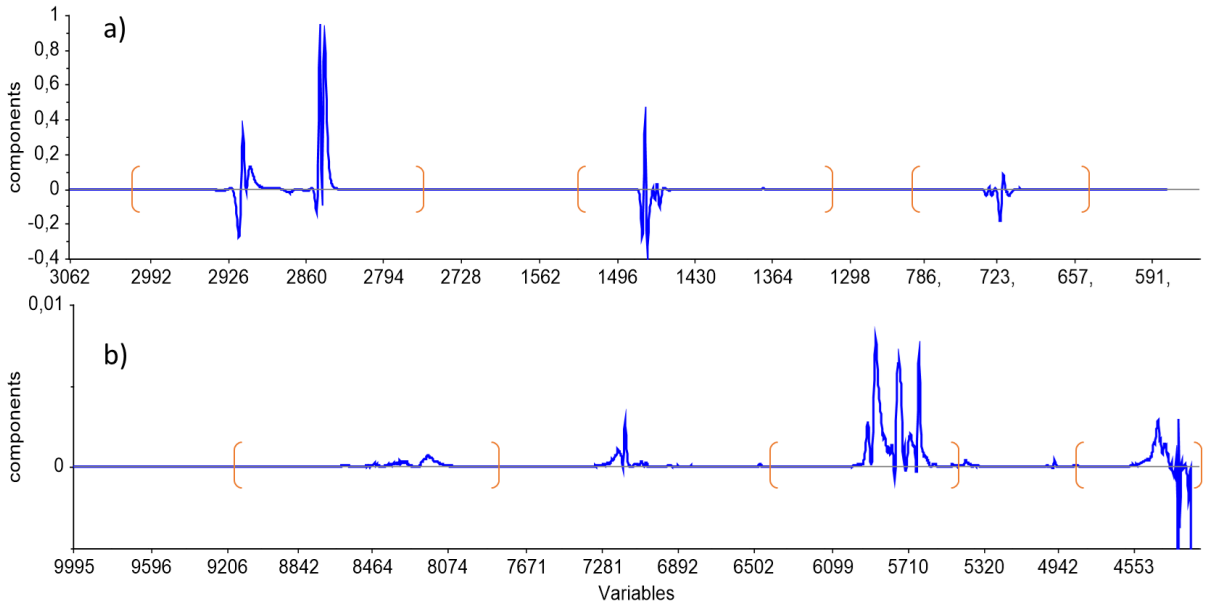

Figure 6. The contribution plot describes how individual variables contribute to the model, 3 spectral regions were clearly highlighted a) in MIR and b) in NIR. Variables represents the wavelength in cm^{-1}. The brackets indicate the wavelength ranges selected to be included in the models.

In the contribution plot for MIR (**Figure 6a**), three spectral regions contribute significantly to the discrimination. In order to improve the model and eliminate the wavelength likely generating noise, we decided to select only the interesting spectral region: the bands from 3000 to 2750 cm^{-1}, from 1500 to 1300 cm^{-1} and from 800 to 630 cm^{-1}. This corresponds well to the main absorption wavelengths of polyethylene (2914 cm^{-1}, 2847 cm^{-1}, 1472 cm^{-1}, 1462 cm^{-1}, 730 cm^{-1} and 718 cm^{-1}) indicated in previous work.[49] For NIR, the contribution plot (**Figure 6b**) made it possible to select the bands from 9000 to 7800 cm^{-1}, from 6400 to 5400 cm^{-1} and from 4800 to 4000 cm^{-1}. Although we observed an absorption between 7500 to 6900 cm^{-1}, this range

was not selected in the model. The NIR model has been improved without the use of this range mainly impacted by the solvent.

3.7.2. Calibration and validation

Using the samples different models were created, six of them are reported in **Table 3**. Since common industrial LLDPEs have a low 1-hexene content of up to 4 mol%, calibrations with a reduced 1-hexene range have also been designed to be more precise. Models [c] for MIR and [f] for NIR, reported in Table 3, were constructed with samples ranging from 0 to 4 mol% of 1-hexene.

Table 3. Processing parameters of six PLS models for MIR and NIR

Model	**IR**	**Sample[a]**	**Spectrum[b]**	**Pre-treatment[c]**	**Range[d] (mol%)**
[a]	MIR	solid	whole	derivative SG	0-21
[b]	MIR	solid	selection	derivative SG	0-21
[c]	MIR	solid	selection	derivative SG	0-4
[d]	NIR	solid	whole	derivative SG	0-21
[e]	NIR	dissolved	whole	derivative SG	0-21
[f]	NIR	dissolved	selection	derivative SG	0-4

[a] solid or dissolved sample in 1,2,4 TCB, [b] whole spectrum or spectral region selection (3000-750, 1500-1300 and 630-800 cm^{-1} for MIR ; 9000-7800, 6400-5400 and 4800-4000 cm^{-1} for NIR), [c] first derivative and Savitzky–Golay smoothing, [d] range of the 1-hexene content in samples used for calibration.

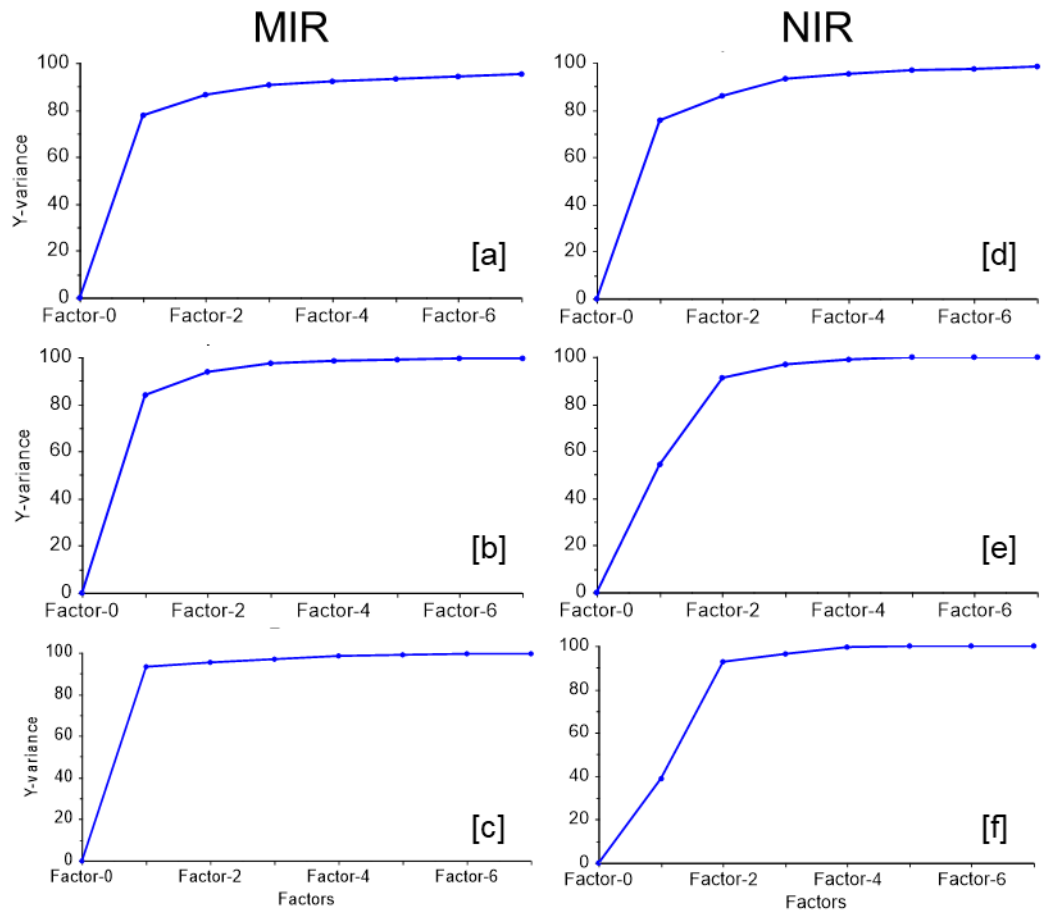

Figure 7. Evolution of performance index (in %) in function of the number of PLS factors for the six models reported in Table 3.

With four factors and a spectral region selection, the performance index plot reached a maximum of 97.7% for MIR (method [b] in **Figure 7**) and a maximum of 97.2% for NIR (method [e] in Figure 7). It was, once again, improved for methods with a reduced 1-hexene content range (method [c] and [f]). The numerical values of the performance index for the different tests are compared in Table 4. We observed that spectral region selection, with superior interpretability, significantly improved performance of the model and produced the lowest prediction error. **Figure 8** shows the calibration curve for the quantification of 1-hexene content using different parameters detailed in Table 3 to construct the regression.

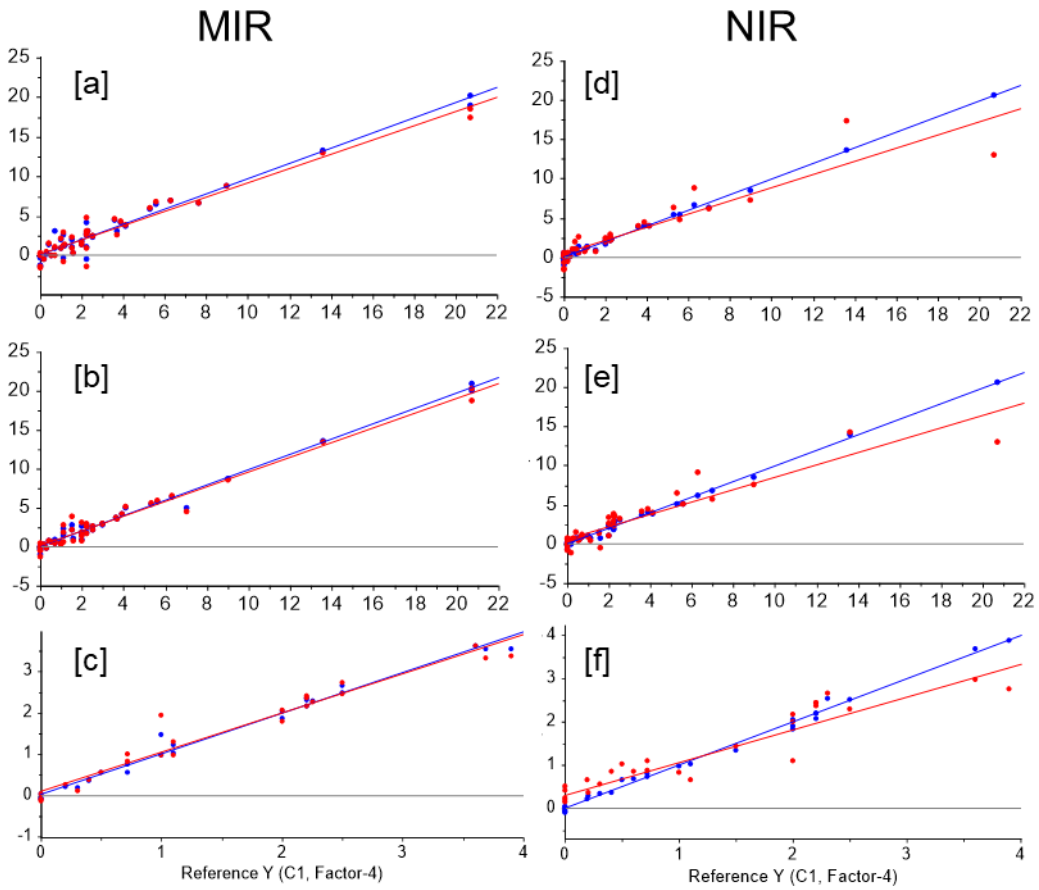

Figure 8. Correlation diagrams between predicted and reference values of the dataset for the six models reported in Table 3 (blue data for calibration and red data for validation). The axes units are expressed in mol% (1-hexene content).

The assessments of the six PLS models are summarized in **Table 4**.

Table 4. Assessment of the PLS models for MIR and NIR

Model	**[a] MIR**	**[b] MIR**	**[c] MIR**	**[d] NIR**	**[e] NIR**	**[f] NIR**
Number of factors	4	4	4	4	4	4
Performance index	97.4	97.7	98.5	91.8	97.2	98.2
RMSEC	0.6	0.5	0.1	1.0	0.3	0.1
r_c^2	0.98	0.99	0.99	0.96	0.99	0.98
RMSEV	0.9	0.6	0.2	1.6	1.7	0.4

r_v^2	0.97	0.98	0.97	0.86	0.85	0.84

The RMSEV values for the MIR model were slightly better than that values of NIR model. Finally, it appears that the methods [b] and [e] were reliable for the determination of the 1-hexene content in copolymers containing high co-monomer content (up to 21 mol%). For lower content the methods [c] and [f] will be the most efficient and suitable. The repeatability and the validity of both methods were evaluated using new samples.

3.8. Repeatability of the model

A repeatability test for the measurement of 1-hexene content using the MIR and NIR methods ([c] and [f]) was performed. An unknown ethylene-1-hexene copolymer was measured 10 times by the same operator, in a short period of time. Afterwards, the PLS models [c] and [f] were applied to all IR spectra to quantify the 1-hexene content.

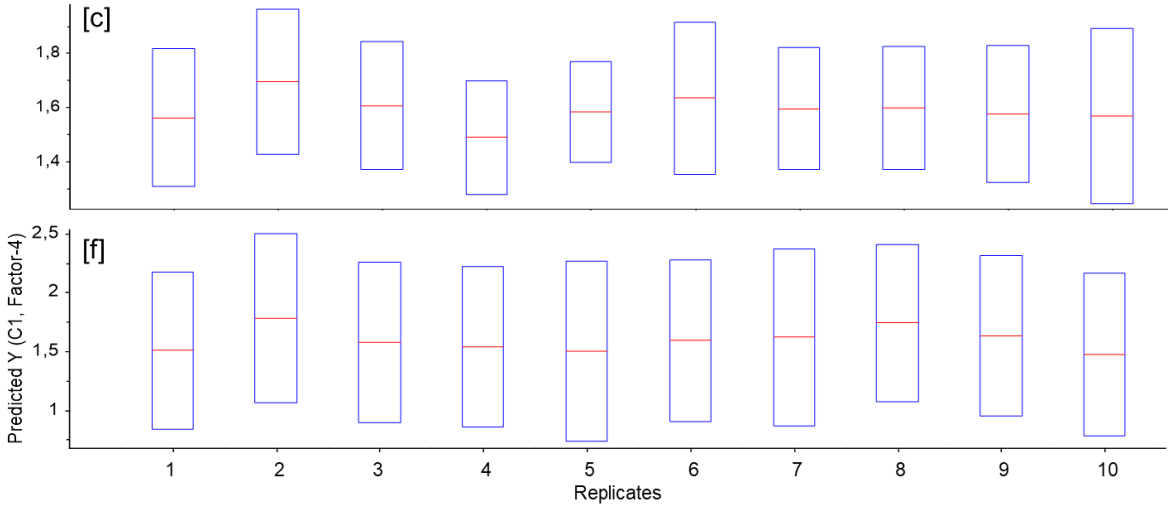

Figure 9. Predicted values (in red) and deviation (in blue) of a repetability test for the MIR and NIR models, quantifiquantion of 1-hexene content (in mol%) for an unknow sample with the method [c] and [f].

A good repeatability of both methods was observed based on the data plot in **Figure 9**. An average of 1.59 mol% with a standard deviation of 0.05 were obtained for MIR method [c] and

an average of 1.60 mol% and standard deviation of 0.08 were obtained for NIR method [f]. Since a very similar average value for both methods and low sigma values were obtained, we concluded that the proposed models were accurate. Furthermore, the values were in good agreement with the 1.50 mol% obtained by NMR. The relative standard deviation (RSD) for each model was calculated using 10 replicates of the same sample. It is reported in **Table 5**.

Table 5. The relative standard deviation of each model determined with 10 replicates of one sample.

Model	**[a] MIR**	**[b] MIR**	**[c] MIR**	**[d] NIR**	**[e] NIR**	**[f] NIR**
RSD	4.9%	3.9%	3.1%	6.8%	6.1%	5.0%

3.9. Validation of the model

With all those observations it seems that the use of the method for the quantification of 1-hexene for an unknown copolymer is appropriate. In order to validate the model in real conditions, four new ethylene-1-hexene copolymers, obtained by Ziegler Natta catalyst, were analysed with both NMR and the proposed NIR and MIR models. The results are given in **Table 6**.

Table 6. Comparison of NMR and IR data of three unknown ethylene-1-hexene copolymers for the validation of the chemometric method.

Sample	1-Hexene [mol%]		
	NMR	MIR method [b] [c]	NIR method [e] [f]
A	0.6	0.7[c]	0.7[f]
B	2.2	2.7[c]	2.8[f]
C	5.3	5.6[b]	5.9[e]
D	10.2	10.1[b]	11.0[e]

[b] prediction value obtained with method [b], [c] prediction value obtained with method [c], [e] prediction value obtained with method [e], [f] prediction value obtained with method [f]

The values calculated by the models all show a bias in the same direction: the predicted results are all higher than the NMR results. This indicates that there is a small source of systematic error in the case of LLDPE obtained with Ziegler Natta catalyst and analyzed by these models. However, the predicted values obtained by IR are quite close to NMR results, which shows that the PLS model can be applied as a routine analysis. Considering this result, we can also conclude that the proposed model is reliable and accurate.

4. Conclusion

In this study a MIR and NIR method combined with PLS modeling was developed for a rapid determination of 1-hexene units in LLDPE. A series of 41 copolymers with a wide variety of chemical composition was synthetized. SEC profiles and TGIC profiles showed that all polymers were quite homogeneous in molar mass and composition. They were then characterized by NMR to determine 1-hexene content, and analysed by MIR and NIR. The IR spectra obtained were exploited using chemometric tools and correlate with NMR results. The PLS method was revealed to be rapid, highly efficient and low-cost for determining the composition of copolymers even if characteristic vibrations of 1-hexene are indistinguishable in the spectrum. The proposed methodology provides also the great advantage of non-destructive measurement. The method is highly satisfactory based on its good repeatability and accurate results. This study shows that chemometric analysis of MIR and NIR spectrum is an easy and a valuable tool to understand the chemical composition of copolymers. The developed models can be applied for routine analysis of unknown samples with satisfactory results.

Acknowledgments: the authors thank the NMR Polymer Center of Institut de Chimie de Lyon (FR5223) for assistance and access to the NMR facilities and Stephane Lebras from Thermo Fisher Scientific for support in IR.

Keywords: infrared; near infrared; ethylene-1-hexene copolymer; LLDPE; chemometrics

Table of Contents

The comonomer content has a strong impact on the properties of LLDPEs. This article describes a rapid investigation method, based on a combination of mid and near infrared spectroscopy and chemometrics tools, for measuring the amount of comonomers. The processing and the assessment of the obtained regression models are discussed and show that the methods are efficient, accurate and fast.

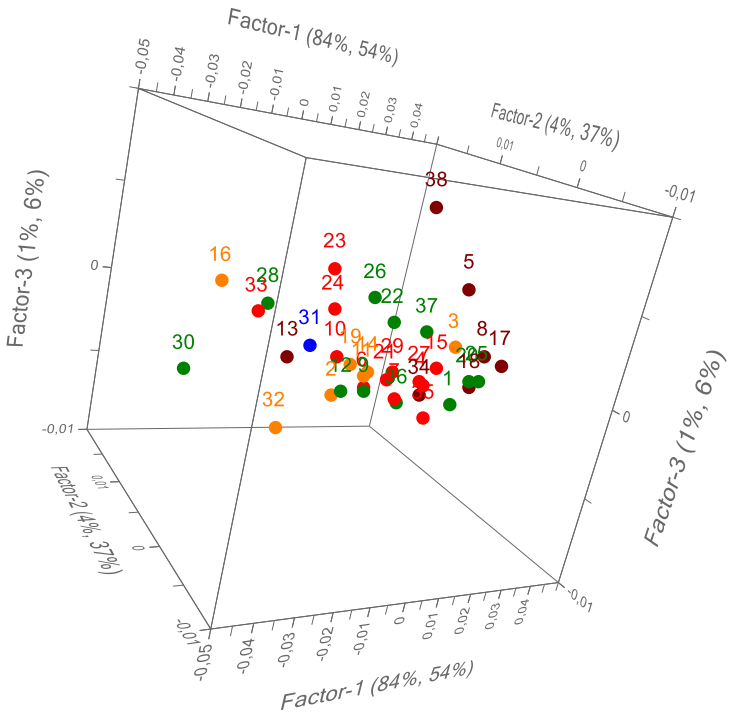
Factor-1 (84%, 54%)
Factor-2 (4%, 37%)
Factor-3 (1%, 6%)
-0,05
-0,04
-0,03
-0,02
-0,01
0
0,01
0,02
0,03
0,04
0,01
0
-0,01
-0,01
0
0,01
Factor-3 (1%, 6%)
Factor-2 (4%, 37%)
-0,01
0
0,01
-0,05
-0,04
-0,03
-0,02
-0,01
0
0,01
0,02
0,03
0,04
Factor-1 (84%, 54%)
38
16
23
5
28
33
24
26
22
37
3
31
13
10
30
8
17
15
29
27
25
46
1
32

[1] R. Mulhaupt, *Macromol. Chem. Phys.* **2003**, *204*, 289.

[2] W. D. Sauter, M. Taoufik, C. Boisson, *Polymers* **2017**, *9*.

[3] M. M. Stalzer, M. Delferro, T. J. Marks, *Catal. Lett.* **2015**, *145*, 3.

[4] M. P. McDaniel, *Adv. Catal.* **2010**, *53*, 123.

[5] V. Kumar, C. R. Locker, P. J. in 't Veld, G. C. Rutledge, *Macromolecules* **2017**, *50*, 1206.

[6] S. Bensason, J. Minick, A. Moet, S. Chum, A. Hiltner, E. Baer, *J. Polym. Sci. Pol. Phys.* **1996**, *34*, 1301.

[7] J. P. Blitz, D. C. McFaddin, *J. Appl. Polym. Sci.* **1994**, *51*, 13.

[8] L. H. Cross, R. B. Richards, H. A. Willis, *Faraday Discuss.* **1950**, *9*, 235.

[9] T. Usami, S. Takayama, *Polym. J.* **1984**, *16*, 731.

[10] C. France, P. J. Hendra, W. F. Maddams, H. A. Willis, *Polymer* **1987**, *28*, 710.

[11] J. C. Randall, *J. Polym. Sci. Pol. Phys.* **1973**, *11*, 275.

[12] D. E. Dorman, E. P. Otocka, F. A. Bovey, *Macromolecules* **1972**, *5*, 574.

[13] W. Liu, P. L. Rinaldi, L. H. McIntosh, R. P. Quirk, *Macromolecules* **2001**, *34*, 4757.

[14] M. E. A. Cudby, A. Bunn, *Polymer* **1976**, *17*, 345.

[15] L. Wild, T. R. Ryle, D. C. Knobeloch, I. R. Peat, *J. Polym. Sci. Pol. Phys.* **1982**, *20*, 441.

[16] L. Wild, *Adv. Polym. Sci.* **1991**, *98*, 1.

[17] L. Wild, C. Blatz, *New Adv. Polyolefins*, Plenum Press, New York, **1993**.

[18] E. Cossoul, L. Baverel, E. Martigny, T. Macko, C. Boisson, O. Boyron, *Macromol. Symp.* **2013**, *330*, 42.

[19] T. Macko, H. Pasch, *Macromolecules* **2009**, *42*, 6063.

[20] B. Monrabal, J. Blanco, J. Nieto, J. B. P. Soares, *J. Polym. Sci. Pol. Chem.* **1999**, *37*, 89.

[21] J. B. P. Soares, S. Anantawaraskul, *J. Polym. Sci. Pol. Phys.* **2005**, *43*, 1557.

[22] T. Macko, R. Bruell, Y. Zhu, Y. Wang, *J. Sep. Sci.* **2010**, *33*, 3446.

[23] B. Monrabal, L. Romero, *Macromol. Chem. Phys.* **2014**, *215*, 1818.

[24] R. Cong, W. de Groot, A. Parrott, W. Yau, L. Hazlitt, R. Brown, M. Miller, Z. Zhou, *Macromolecules (Washington, DC, U. S.)* **2011**, *44*, 3062.

[25] B. Monrabal, *Adv. Polym. Sci.* **2013**, *257*, 203.

[26] R. Chitta, T. Macko, R. Bruell, C. Boisson, E. Cossoul, O. Boyron, *Macromol. Chem. Phys.* **2015**, *216*, 721.

[27] F. Brunel, O. Boyron, A. Clement, C. Boisson, *Macromol. Chem. Phys.* **2019**, *220*, 1800496.

[28] E. Roumeli, A. Markoulis, T. Kyratsi, D. Bikiaris, K. Chrissafis, *Polym. Degrad. Stabil.* **2014**, *100*, 42.

[29] T. Usami, Y. Gotoh, S. Takayama, H. Ohtani, S. Tsuge, *Macromolecules* **1987**, *20*, 1557.

[30] S. Duc, N. Lopez, *Polymer* **1999**, *40*, 6723.

[31] O. Boyron, T. Marre, A. Delauzun, R. Cozic, C. Boisson, *Macromol. Chem. Phys. 2019*, 1900162.

[32] J. L. Koenig, M. K. Antoon, *Appl. Opt.* **1978**, *17*, 1374.

[33] C. Baker, P. David, W. F. Maddams, *Makromol. Chem.* **1979**, *180*, 975.

[34] J. B. Huang, J. W. Hong, M. W. Urban, *Polymer* **1992**, *33*, 5173.

[35] F. M. Mirabella, *Appl. Spectrosc. Rev.* **1985**, *21*, 45.

[36] K. Sahre, U. Schulze, K.-J. Eichhorn, B. Voit, *Macromol. Chem. Phys.* **2007**, *208*, 1265.

[37] A. Cherfi, G. Févotte, *Macromol. Chem. Phys.* **2002**, *203*, 1188.

[38] M. P. B. Van Uum, H. Lammers, J. P. De Kleijn, *Macromol. Chem. Phys.* **1995**, *196*, 2023.

[39] L. M. Santos, M. J. Amaral, C. Dariva, E. Franceschi, A. F. Santos, O. Boyron, T. F. L. McKenna, *Macromol. React. Eng.* **2017**, *11*, 1700007.

[40] E. Caro, E. Comas, *Talanta* **2017**, *163*, 48.

[41] M. A. McRae, W. F. Maddams, *Makromol. Chem.* **1976**, *177*, 449.

[42] K. Sano, M. Shimoyama, M. Ohgane, H. Higashiyama, M. Watari, M. Tomo, T. Ninomiya, Y. Ozaki, *Appl. Spectrosc.* **1999**, 53, 551.

[43] M. Shimoyama, T. Ninomiya, K. Sano, Y. Ozaki, H. Higashiyama, M. Watari, and M. Tomo, J. Near Infrared Spectrosc. 1**998**, 6, 317.

[44] R. W. Gerlach, B. R. Kowalski, H. O. A. Wold, *Anal. Chim. Acta* **1979**, *112*, 417.

[45] P. Bastien, V. E. Vinzi, M. Tenenhaus, *Comput. Stat. Data Anal.* **2005**, *48*, 17.

[46] B. S. Dayal, J. F. MacGregor, *J. Chemometr.* **1997**, *11*, 73.

[47] F. Lindgren, P. Geladi, S. Wold, *J. Chemometr.* **1993**, *7*, 45.

[48] S. Rännar, F. Lindgren, P. Geladi, S. Wold, *J. Chemometr.* **1994**, *8*, 111.

[49] O. Boyron, B. MacQueron, M. Taam, J. Thuilliez, C. Boisson, *Macromol. Chem. Phys.* **2018**, *219*, 1700609.

[50] W. Kaminsky, *Macromolecules* **2012**, *45*, 3289.

[51] W. Kaminsky, A. Funck, H. Hähnsen, *Dalton Trans.* **2009**, 41, 8803.

[52] H. Sinn, W. Kaminsky, H.-J. Vollmer, R. Woldt, *Angew. Chem. Int. Ed.* **1980**, *19*, 390.

[53] F. Prades, J.-P. Broyer, I. Belaid, O. Boyron, O. Miserque, R. Spitz, C. Boisson, *Acs Catalysis* **2013**, *3*, 2288.

[54] J. C. Randall, J. *Macromol. Sci. Polymer Rev* **1989**, *29*, 201.

[55] N. Inwong, S. Anantawaraskul, J. B. P. Soares, A. Z. Al- Khazaal, *Macromol. Symp.* **2015**, *356*, 54.

[56] B. Monrabal, N. Mayo, R. Cong, *Macromol. Symp.* **2012**, *312*, 115.

[57] A. Z. Al-Khazaal, J. B. P. Soares, *Macromol. Chem. Phys.* **2014**, *215*, 465.

[58] A. Alghyamah, J. B. P. Soares, *Ind. Eng. Chem. Res.* **2014**, *53*, 9228.

[59] F. M. Rugg, J. J. Smith, L. H. Wartman, *J. Polym. Sci.* **1953**, *11*, 1.

[60] A. H. Willbourn, *J. Polym. Sci.* **1959**, *34*, 569.

[61] S. Krimm, C. Y. Liang, G. B. B. M. Sutherland, *J. Chem. Phys.* **1956**, *25*, 549.

[62] K. Rossmann, *J. Chem. Phys.* **1955**, *23*, 1355.

[63] M. Mizushima, T. Kawamura, K. Takahashi, K.-h. Nitta, *Polym. J.* **2011**, *44*, 162.

[64] S. Watanabe, J. Dybal, K. Tashiro, Y. Ozaki, *Polymer* **2006**, *47*, 2010.

[65] A. Höskuldsson, *J. Chemometr.* **1988**, *2*, 211.

[66] J. Luo, K. Ying, J. Bai, *Signal Process.* **2005**, *85*, 1429.

[67] A. Savitzky, M. J. E. Golay, *Anal. Chem.* **1964**, *36*, 1627.

[68] P. A. Gorry, *Anal. Chem.* **1990**, *62*, 570.